Environmental Sciences Europe

RESEARCH

Open Access

Microplastic clouds in rivers: spatiotemporal dynamics of microplastic pollution in a fluvial system

Alexia Balla[1*], Ahmed Moshen[1,2] and Tímea Kiss[3]

Abstract

Background The microplastic transport of rivers is a complex spatiotemporal process; however, only limited knowledge exists on it, making its monitoring complicated. The study aimed to analyze the spatial and temporal dynamics of suspended sediments and microplastics based on measurements (1) every five days for 2 years at one site and (2) annual repetition at 29 sites along the 750-km-long Tisza River for 3 years. Water samples were taken by pumping (1 m^3). Machine learning algorithms were applied to Sentinel images to analyze the spatiality of sediment transport.

Results In the Tisza River (Central Europe), the microplastic concentration (MPC_{mean}: 35 ± 27 item/m^3) and the suspended sediment concentration (SSC_{mean}: 60 ± 57 g/m^3) showed high temporal variations. During low stages, the concentrations dropped as most transported sediments were deposited on the bottom. These sediments, including microplastics, were remobilized during flood waves, thus, higher MPC and SSC were measured. The first flood wave after a low-stage period had the highest concentrations. The increased transport capacity of the river during floods created large-scale suspended sediment and microplastic waves with increased concentrations. The mean MPC gradually increased between 2021 (19 ± 13.6 item/m^3) and 2022 (23.7 ± 15.8 item/m^3), and then it more than doubled (2023: 57 ± 44.8 item/m^3). The tributaries acted as suspended sediment and microplastic conveyors.

On the Sentinel images, medium-scale clouds were identified, with the suspended sediment clouds being more pronounced than microplastic clouds. Fewer and longer clouds appeared during low stages, separated by clearer water bodies. During flood waves, shorter clouds were detected. The tributaries with increased suspended sediment and microplastic transport created well-distinguishable clouds in the main river.

Conclusions Identifying suspended sediment and microplastic clouds in a river could support more precise monitoring. The hydrological background of the monitoring and the existence of these clouds should be considered, as sampling from clouds with increased SSC and MPC provides different data than sampling from the clearer water bodies between two clouds.

Keywords Microplastic monitoring, Suspended sediment monitoring, Microplastic cloud, Sediment cloud, Flood, Low stage

*Correspondence:
Alexia Balla
balla.alexia@stud.u-szeged.hu
Full list of author information is available at the end of the article

Graphical Abstract

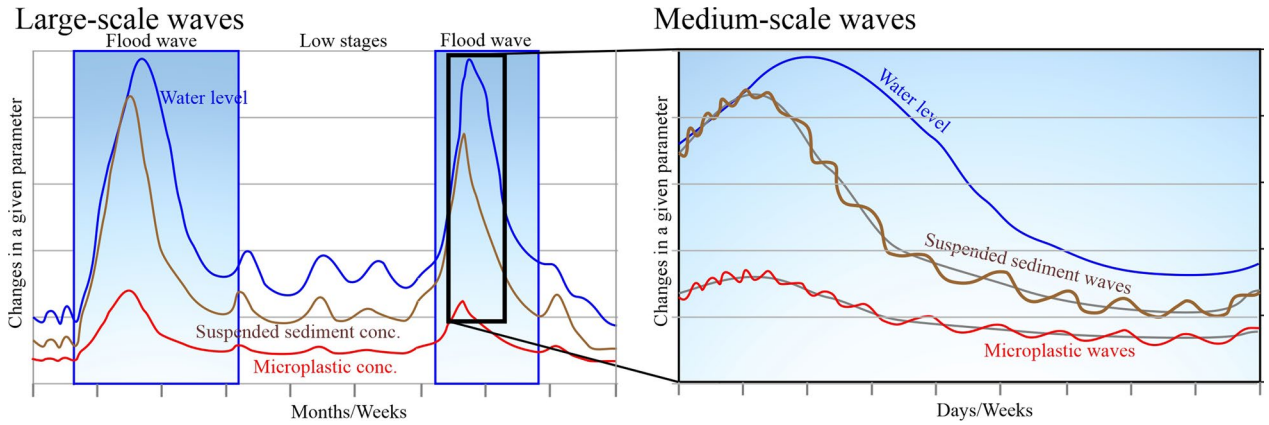

Introduction

Microplastics (MP: < 5 mm) became a major physical contaminant of surface waters from various sources. One of the most important sources is inadequately treated or untreated wastewater [9, 41, 63], although treated wastewater also contains 10–20% MPs that are released to the environment via effluent waters [15, 17, 18, 58, 66]. Other sources of MPs include illegal landfills, from where the fragmented plastics could be transported to surface waters by runoff [18, 66]. The urban environment is also an important MP source due to the weathering of road paint, plastic surfaces, traffic, and construction [1, 9, 21]. Furthermore, certain agricultural activities (e.g., plastic greenhouses, plastic irrigation, and storage equipment) can also contribute large amounts of MP to the environment [25, 57]. Sewage sludge, a byproduct of wastewater treatment, could be used in agriculture as a fertilizer. However, despite being free of toxins and heavy metals, it can contain many MPs [26, 40]. The MPs originating from various sources are ultimately transported to rivers [25] through surface runoff [5, 20] or atmospheric deposition [5, 16]. Thus, even remote areas such as floodplains and seas can be contaminated, endangering wildlife and food safety.

The number of MP studies is increasing; however, it is difficult to compare results (Table 1) for several reasons. One of the greatest problems is the sampling methodology, as the tested volume of water is not uniform. To determine the microplastic concentration (MPC) in a given volume, a wide range of equipment is used, from pumps (sampled volume: 1 m^3; [54]) to jars (1.5 L, [46]); thus, the volume of the sampled water varies by three orders of magnitude. In addition, stationary driftnets [39] or floating manta nets [20] are also applied. These methods make the MPC calculation much more uncertain, as the amount of MP at a given point of a cross-section differs from the real amount that passes through the cross-section of a river [41].

The comparability of the results becomes even more complicated if the environmental conditions of the sampling (e.g., site selection, hydrological background) are considered. As the MPs are transported similarly to suspended sediments (SS), the knowledge of SS monitoring could be applied in MP studies. As the suspended sediment concentration (SSC) and MPC vary spatially, careful sampling point selection is needed. Some studies on the vertical distribution of SSC and MPC have already proved that particles in the cross-section of a river are not evenly distributed. Greater MPC was measured close to the surface and to the bottom of the channel in connection to their differences in density [41], whereas the greatest SSC was at the bottom of the channel [33]. Thus, the sampling depth is an important parameter of the MP surveys, though it is often neglected. The mixing of waters from tributaries, canals, or wastewater treatment plants should also be considered. The water bodies with different origins could contain different amounts of MP and SS [42, 46], thus, their mixing processes could influence the results of an MP survey downstream of confluences and inlets. Still, there is hardly any MP research on a longer river or an entire river section (except [28], which aimed to analyze the spatial distribution of MPC and its temporally changing influencing factors.

As the analysis of MPC is very costly and labor intensive, the existing knowledge on SS transport could be implemented in MP studies, and the natural SS could be used as a proxy to model MP transport [46]. The transport of MP grains is influenced by similar factors as SS

Table 1 Examples of different approaches in microplastic research. The studies considerably differ in their spatial and temporal repetitions, and applied sampling methods

Author	River (Country)	Survey type	Number of sites	Used equipment	Volume of sampled water	Converted microplastic concentration	Possible MP sources
Lechner et al. [39]	Danube (Austria)	Spatio-temporal	3–4	stationary driftnet	Not reported	317 item/1000 m^3	Plastic production
Faure et al. [20]	Rhone (Switzerland)	Spatio-temporal	6	floating manta net	360 m^3	7 item/m^3	Surface runoff
Estahbanati et al. [18]	Ratian (USA)	Spatial	8	plankton nets	1.3–3.5 m^3	24.0–71.7 item/m^3	Sewage, effluent, litter degradation
Wang et al. [66]	Wuhan (China)	Spatial	16	teflon pump	20 L	1660–8925 item/m^3	Municipal effluent
Schmidt et al. [59]	Teltow Canal (Germany)	Spatio-temporal	10	Niskin bottle/ plankton nets	Average 12.4 L	0.01–95.80 item/L	Sewage, effluent, surface runoff
Rodrigues et al. [54]	Antuã River (Portugal)	Spatio-temporal	6	motor water pump	1.2 m^3	71–1265 item/m^3 58–193 item/m^3	Industry, urbanization and WWTP
Di et al. [15]	Yangtze (China)	Spatial	29	teflon pump	25 L	1597–12611 item/m^3	Sewage, effluent, litter degradation
Lahens et al. [36]	Saigon and canals (Vietnam)	Spatio-temporal	6	nets	0.3 L / not reported	172000–519000 item/$m^3$and 10–223 item/m^3	Industrial and sewage effluent, litter degradation
Dris et al. [16]	Seine (France)	Spatio-temporal	3	collection funnel/ automatic samplers	182–200 m^3	0.28–0.47 item/m^3	Sewage effluent, atmospheric fallout, urban runoff
			4		0.43–2.0 m^3	4–108 item/m^3	
Eo et al. [17]	Nakdong (South Korea)	Spatio-temporal	9	stainless steel beaker / submersible pump	100L	293–4760 item/m^3	WWTP
Scherer et al. [58]	Elbe (Germany)	Spatial	10	Apstein plankton net	3.2–32.7 m^3	5.57 ± 4.33 item/m^3	Sewage effluent, industrial emission
Chen et al. [8]	Langat (Malaysia)	Spatio-temporal	8	sampling bottle	2 L	4.39 ± 5.11 item/L	Domestic wastewater discharge
Shekoohiyan and Akbarzadeh [61]	Jajroud (Tehran)	Temporal	7	glass container	2 L	12.14 ± 10.07 particles/L	Wastewater
Forrest and Vermaire [22]	Ottawa (Canada)	Spatio-temporal	105	manta net	20,000–163,000 L	0.050–4.955 p/m^3	atmospheric fallout, WWTP
Zhao et al. [71]	XJ River (China)	Spatio-temporal	21	stainless steel samplers	2.5 L	0.72–18.6 (7.32 ± 2.36) items/L	WWTP, anthropogenic sources
Idowu et al. [29]	Osun (Nigeria)	Spatial	5	amber bottles	2.5 L	3791 ± 88 to 22079 ± 134 particles/L	plastic waste
Gonzalez-Salidas et al. [24]	Besòs and Tordera (Spain)	Spatial	15 and 14	metal bucket, 50 µm sieve	100 L	4.40 ± 3.90/L 2.61 ± 1.78/L	Industrial, WWTP

transport [8, 35, 46, 50] due to their similar grain-size range [10], however, there are also differences between their transport. The MP grains have a significantly wider density range, they are easily deformed and fragmented [64], besides, the aggregate formation of MPs and natural sediments [25] increases the rate of MP deposition [42]. These differences may explain some contradictory results between MP and SS concentrations [8, 51].

The MP and SS transport varies in different hydrological situations, as demonstrated by Mohsen et al. [48] applying a long and detailed survey. The study revealed that a negligible relationship ($\rho = -0.04$; $p = 0.728$) exists between SSC and MPC at low water stages, but the relationship becomes stronger ($\rho = 0.72$; $p < 0.001$) during flood waves, especially at rising limb and peak of the floods ($\rho = 0.\ 72$; $p < 0.001$). The stronger relationship

during flood waves was explained by their similar transport mechanism though, during low stages, the more efficient deposition of the MPs explains the weak relationship between MP and SS [35]. These differences should be considered during sampling campaigns, still, only a limited number of studies mention the hydrological background of the given study. The situation becomes even more complex if it is considered that sampling is much simpler and less dangerous during low stages; therefore, probably most of the studies are performed during low stages. Therefore, it is necessary to study the link between SSC and MPC during low stages and to analyze the low-stage circumstances in greater detail.

Based on our field experiences, we hypothesized that the SSC and MPC of rivers are not homogenous, as water bodies with higher concentrations develop and these suspended particles appear like "clouds" in the river. We saw such sediment clouds with higher concentrations, especially during low stages when the flow velocity was low ($\leq$0.1 m/s) and turbulence was limited. These MP and SS clouds could be associated with temporal MP and SS inputs from tributaries (in the form of small flood waves) or influent waters (e.g., wastewater inflow). According to our hypothesis, water bodies with lower concentrations separate clouds with high MPC and SSC. The clouds migrate downstream, resulting in large variability in the amount of MP within the water system during low flow conditions.

Therefore, the objective of the study was to investigate the temporal and spatial factors influencing the SSC and MPC in the fluvial system of the Tisza River (Central Europe). The aims of the research were (1) to analyze the temporal correlation between SSC, MPC and hydrology based on a 5-day return period monitoring for two years at one site; (2) to study the spatial changes in MPC along the Tisza River and in its main tributaries during three consecutive years at low water stages; (3) to identify the hydrological and hydro-morphological factors influencing the MPC; (4) identify SS and MP clouds on Sentinel images and compare their characteristics in different hydrological situations. A significant strength of the study is the scale of the sampling. Sampling was performed (1) every 5 days at one site for 2 years and (2) along the entire length of the river (745 km) every 50 km for 3 years. Thus, the study provides insight into plastic transport on a medium-sized transboundary lowland river with different waste management policies, taking into account hydrology and pollution clouds.

Study area

The study was carried out in the fluvial system of the Tisza River (Central Europe). The catchment (157,000 km^2) is shared by five countries (Ukraine, Romania, Slovakia, Hungary, and Serbia), with different natural geographic characteristics, waste and wastewater treatment practices. In the first year (2021), the entire length of the Tisza (946 km) was sampled. In the subsequent years, water samples were collected just along the Hungarian and Serbian sections of the Tisza (745 km), as the Ukrainian sites were skipped because of the war (Fig. 1). The Tisza was divided into five sections (S1-S5) according to the hydrological and morphological characteristics. Their detailed description is in Appendix A.

Based on the long-term record, overbank floods of the Tisza were typical from early spring to early summer, when snow melts in the mountainous areas were combined with spring rains [38]. However, in the last decade, these floods were replaced by smaller, bankfull floods, mainly in winter. Besides, on the smaller sub-catchments, small summer flood waves developed driven by heavy thunderstorms associated with Mediterranean cyclones. Formerly, low water levels were typical between August and February, but this period has shifted and become longer (from spring to late autumn). There are great differences between flood waves and low stages, as on the Upper Tisza at Vásárosnamény (site "h"), the difference in water levels is 991 cm, and the largest discharge (Q_{max} = 2160 m^3/s) is 21 times greater than the lowest discharge (Q_{min} = 104 m^3/s). These extreme values slightly increase towards downstream, as on the Lower Tisza at Szeged (site "v"), the difference in water levels is 933 cm, and it is 13 times between the characteristic discharges (Q_{max} = 3790 m^3/s; Q_{min} = 296 m^3/s).

The first (and last) system-scale sediment measurement was carried out in the 1960s [6]. Ever since, only suspended sediment has been measured on a monthly basis at five sites. The SS transport of the Tisza increases downstream, being 0.9 million m^3/y at site "h" and 12.2 million m^3/y at site "v". On the contrary, the bedload decreases from 22,600 m^3/y to 9000 m^3/y (Bogárdi, 1971). Probably, these data are no longer valid as dams were built on the Tisza at Tiszalök (1959), Kisköre (1973), and Novi Becej (1976). Their reservoirs are efficient sediment traps, each trapping 600–900 thousand m^3 of sediment annually [12, 53]. Based on the monthly measurements, the SSC ranges from 113 to 1553 g/m^3 at Szolnok and 157 to 1880 g/m^3 at Szeged (2015–2020). The highest SSCs (138–248 g/m^3) appear before the peak of floods, but during low stages, most of the transported SS is deposited on the bottom [11].

Materials and methods

The study followed two spatiotemporal approaches. The intra-annual temporal changes in SSC and MPC were analyzed during a two-year-long campaign (May 2021–May 2023): water samples were collected every 5 days

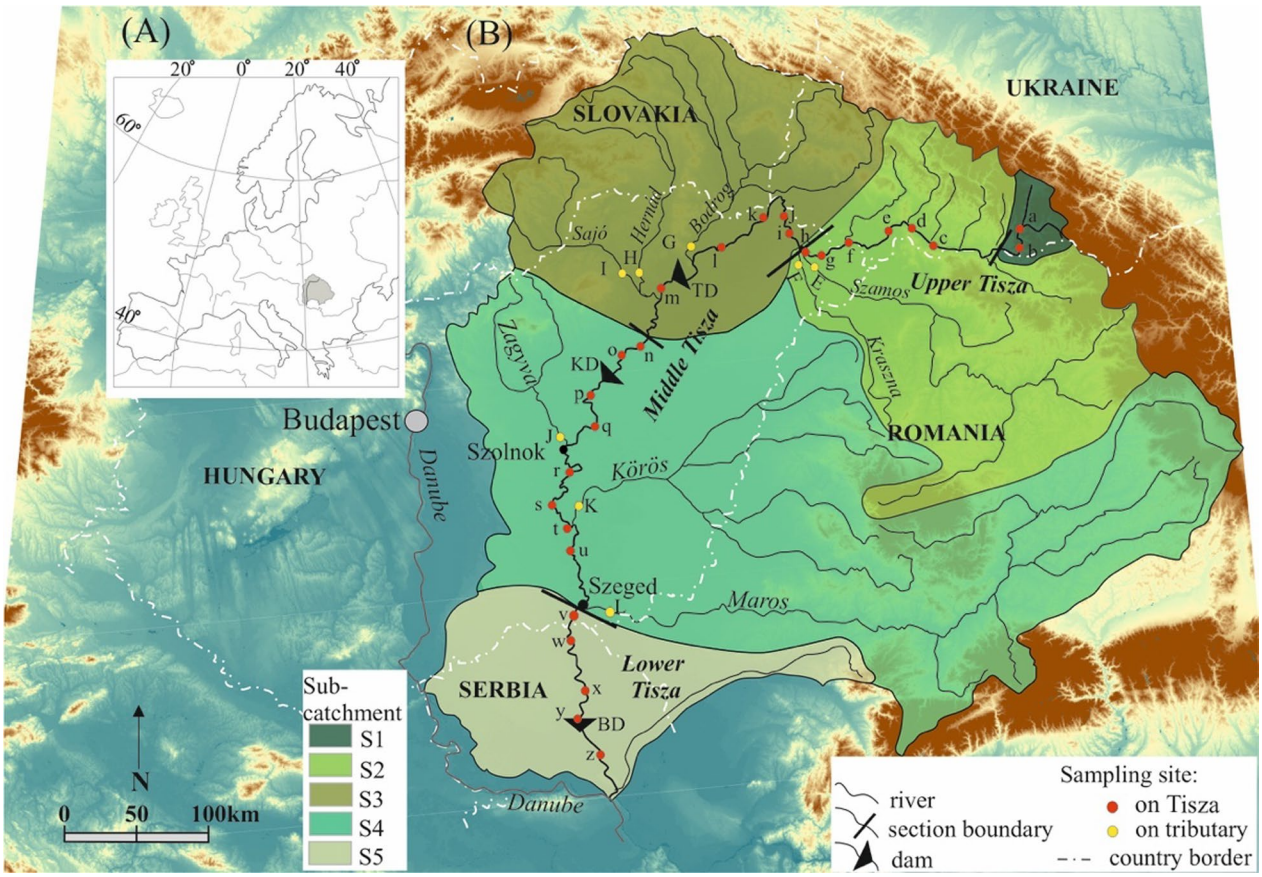

Fig. 1 The fluvial system of the Tisza was divided into five sections (S1–S5). Water samples (a-z and E–L) were collected from 29 sites. The flow conditions of the Tisza are influenced by the Tiszalök Dam (TD), Kisköre Dam (KD), and Novi Becej Dam (BD)

at one site ("u": Mindszent). This set of data revealed the connection between hydrology, SS transport, and MPC.

The spatial changes in MPC and SSC were studied through water samples taken ca. every 50 km along the Tisza River and ca. 20 km upstream of the confluence of the main tributaries (Fig. 1). Sampling was performed in three subsequent years, during summer at low stages. In the first year (2021), five water samples were collected in the Ukrainian section; but sampling in 2022–2023 had to be skipped due to the war. In the Hungarian and Serbian sections of the Tisza, 21 samples were taken each year. The tributaries were surveyed in 2021–2023, providing 8–8 samples. MP data from the 2021 and 2022 sampling campaigns have been published [4].

Water sample collection

Unfiltered water samples (1.5 L) were collected at each point, ca. 2–3 m offshore to analyze SSC. Sampling for MP analysis was carried out at the same point by pumping 1.0 m^3 from a depth of 10–20 cm. The water was filtered through metal sieves (200 and 90 µm); only MP particles larger than 90 µm were collected. The samples were washed into glass containers and transported to the laboratory.

Sample preparation for suspended sediment concentration analysis

The SSC was determined by evaporating water (100 °C) from the collected water samples, adopting the ISO 4365 (A) and ASTM D3977-97 (A) standards [3]. The residual dry matter was weighed on an analytical scale. The SSC was expressed in g/m^3.

Sample preparation for microplastic concentration analysis

The water samples were treated with 30 ml hydrogen peroxide (30%) for 24 h at room temperature (25 °C) following Yang et al. [69] to decompose the organic matter. The remaining samples were washed into Petri dishes. MP particles were identified and counted using an Ash Inspex II digital microscope at 60 × magnification [28]. An item was identified as an MP if (1) lacked typical organic structure, (2) reacted in contact with a hot needle [2, 14, 45]; (3) it retained its rigid shape when moved; and (4) it had a particular color (e.g., red,

blue) or shape (e.g., spherical, irregularly fragmented) [28, 31, 68]. Identified MPs were categorized as fibers (colored and non-colored), fragments, and spheres. MP content was expressed in item/m^3.

FTIR measurements were performed to verify the identification accuracy using an ATR-FTIR Shimadzu Infinity 1 s device in the range of 400–4000 cm^{-1} and a resolution of 4 cm^{-1}. The Shimadzu Standard Library database was used to identify the particles. Scores greater than 850 were considered valid [52]. Out of the analyzed 72 particles, 82% were identified as plastic (e.g., polyethylene, polyethylene terephthalate, polypropylene, polyamide, polyester, and polystyrene), and 18% were non-plastic (e.g., carnauba wax, cellulose, hair, and glass).

Only glass and metal instruments were used to avoid contamination during field and laboratory work, and a lab coat made of natural materials was worn. The number of procedure steps was minimized, and samples were always covered between each step to exclude contamination from air deposition. Every fourth sample was a blank to detect background contamination. The blank samples contained 3 ± 2 MP item/sample on average, and the number was subtracted from the MP content of the processed samples.

Remote sensing of suspended sediment and microplastic concentrations

The in-situ, point-like measurements have limited spatial extensibility; therefore, satellite images were employed to provide a synoptic view of the spatial distribution of SSC and MPC in the Tisza. Artificial neural network-based SSC and MPC concentration models developed by Mohsen et al. [46] were applied to reveal the spatial distribution of both variables at selected sites. The models were developed based on intensive spatiotemporal measurements of SSC and MPC in the Tisza, along with synchronous Sentinel-2 and PlanetScope images, and by integrating machine learning algorithms (for details, please check [46]).

Two sites were selected to model the spatial distribution of SSC and MPC. The confluence of the Tisza and Sajó Rivers (485–478 r km) and an 8.3 km long reach at Mindszent ("u"). At the confluence site, the mixing of a small flood wave from a tributary with the main river was analyzed in detail during the low stage. A tributary does not influence the flow conditions at Mindszent; thus, the spatial and temporal distributions of SSC and MPC were analyzed during various hydrological conditions. To analyze the downstream changes in SSC and MPC, the results of the model were extracted from the centerline of the river.

Hydrological data

Daily water stage data are available at several gauging stations but not from all sampling sites. The water level (H_0) on the day of the sampling was recorded, and then, the water level changes in the previous day (H_1) and 21 days (H_{21}) were calculated. The data were provided by the Lower Tisza District Water Directorate (ATIVIZIG).

Statistical analysis

The Spearman's rank-order correlation test was applied to evaluate the strength of correlation between SSC, MPC, and water stages (H). This test was chosen since the collected data for these variables violated the assumption of normality and equal variance (Shapiro–Wilk normality test; $p < 0.05$). Longitudinal correlations were revealed for the Tisza over the 3 years (2021, 2022, and 2023) and for the sampled tributaries in 2022 and 2023. Also, the temporal correlation between SSC and MPC was investigated in detail at the temporal monitoring site ("u"). This detailed dataset lets us evaluate the effect of various hydrological conditions (i.e., low stages and rising, peak, and falling phases of flood waves) on SSC and MPC. Correlation strength was classified according to Dancey and Reidy [13].

Additionally, the Kruskal–Wallis H and post hoc tests were applied to uncover the statistical differences in SSC and MPC among (1) the results of the three years (2021–2023) in the Tisza, (2) the two measured years (2022 and 2023) in the tributaries, and (3) the Tisza and its tributaries in the common survey years (2022 and 2023).

Results

Temporal correlation between hydrology, suspended sediment, and microplastic concentrations based on frequent measurements at one site

The temporal changes in MPC and SSC of water samples were studied at site "u" (Mindszent). The data refer to their characteristic temporal variations simultaneously with hydrological changes (Fig. 2). During the measurements (May 2021–ay 2023), the water level varied between −31 and 615 cm, so the absolute water level difference was 646 cm. The low-stage periods ($H \leq 100$ cm) lasted from mid-summer to early autumn, but they were interrupted by small flood waves (9 times) initiated by heavy rainstorms on some sub-catchments. Medium flood waves (10 times) occurred from December to May, but they reached mostly just the bankfull level. Only two medium floods entered the floodplain in May 2021 (H_{max}: 564 cm) and March 2023 (H_{max}: 614 cm). In comparison, larger flood waves were recorded in the early twenty-first

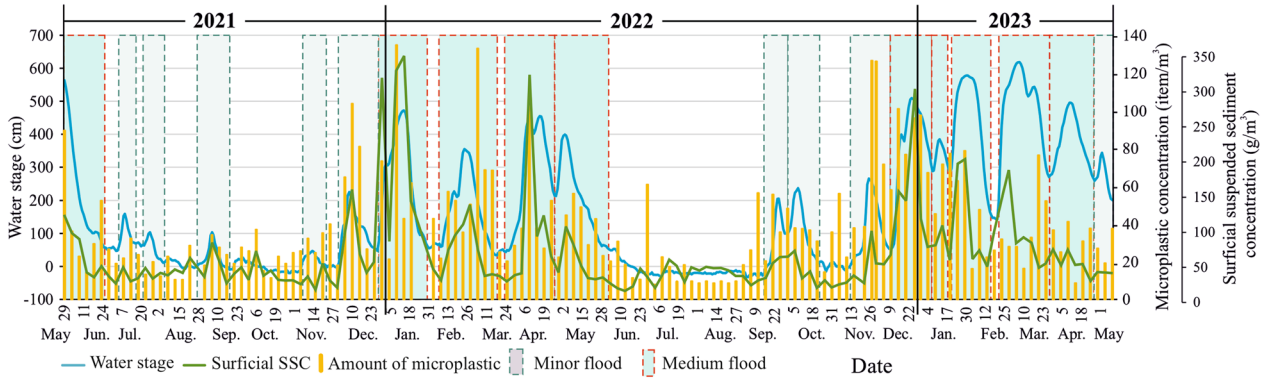

Fig. 2 Temporal changes in daily water stages, suspended sediment, and microplastic concentrations during two years (May 2021–May 2023) at Mindszent (site "u"), Hungary

century. They were up to 400 cm higher (H_{max}: 1062 cm) than the medium floods in the monitored period.

During the monitored period, the SSC fluctuated between 11 and 323 g/m^3 (SSC_{mean}: 60 ± 57 g/m^3) and the MPC was between 2 and 129 item/m^3 (MPC_{mean}: 35 ± 27 item/m^3). They followed a similar pattern as the hydrograph. Accordingly, the lowest concentrations occurred during low stages (SSC_{low}: 34 ± 14 g/m^3; MP_{low}: 21 ± 16 item/m^3) and increased during minor floods. However, the increase in SSC was just by one-third (SSC_{minor}:45 ± 27 g/m^3), whereas the MPC almost doubled (MP_{minor}: 41 ± 30 item/m^3). During medium floods, both variables increased, but the SSC reflected much more dynamic growth, as it further increased by 116% (SSC_{medium}: 97 ± 75 g/m^3) and the MPC just by 15% (MP_{medium}: 47 ± 27 item/m^3).

A strong positive ($\rho = 0.6$) correlation between SSC and MPC was revealed (Fig. 3A). However, the separation of the hydrological conditions revealed that a very strong positive correlation ($\rho = 0.7$) existed during flood waves

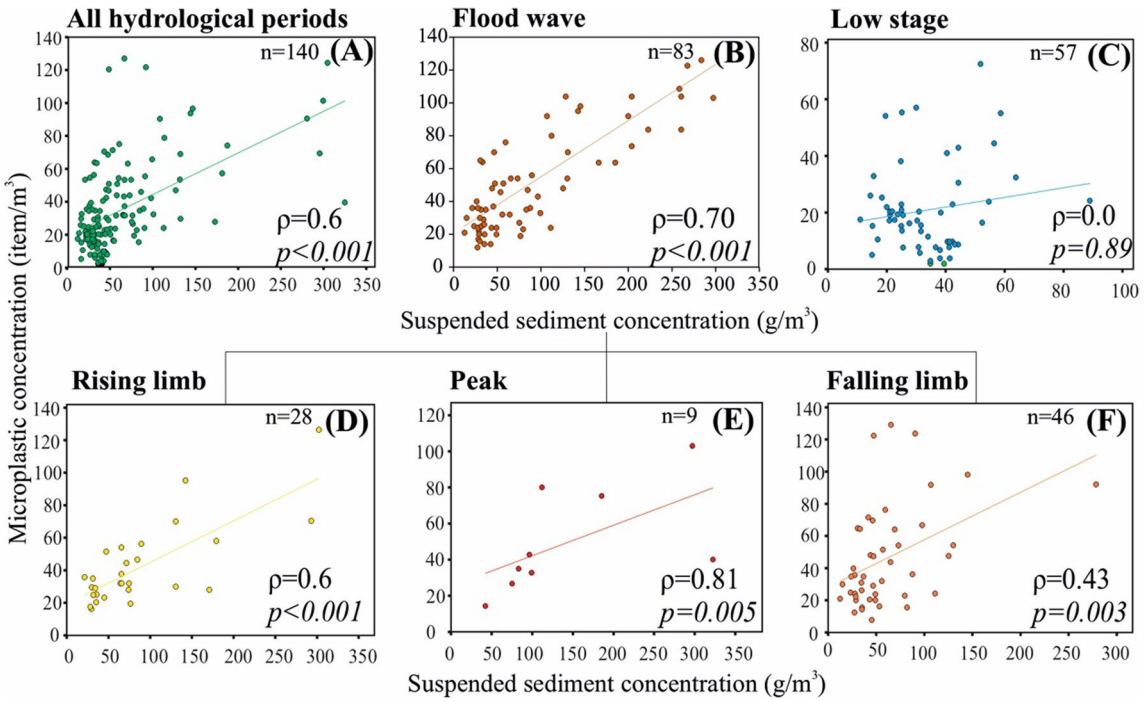

Fig. 3 Correlation between suspended sediment and microplastic concentrations in the water of the Tisza at the monitoring site of Mindszent based on two years of measurements (May 2021–May 2023). The correlation is depicted across all hydrological conditions (**A**), during floods (**B**), and low stages (**C**). Within the different phases of the floods (**D**–**F**), the correlation was also different

and negligible correlation ($\rho = 0.0$) during low stages (Fig. 3B, C). Also, within the flood waves, the correlation varied from strong during the falling ($\rho = 0.43$) and rising ($\rho = 0.60$) phases to very strong ($\rho = 0.81$) during the peak phase (Fig. 3D–F).

Spatial changes in microplastic concentration of the water

In the first year (2021), MPC in the water of the Tisza varied between 0 and 42 item/m^3 (MPC$_{mean}$: 19 ± 13.6 item/m^3) (Fig. 4). There were five out of 26 sites where the MPC was higher than ≥ 30 item/m^3 (Fig. 5); thus, strong or worse MP pollution was measured in 19% of the sites. The only extremely polluted site was in Ukraine ("b": 61 item/m^3). Moderately contaminated sites were the most frequent (35%), but slightly (27%) polluted sites were also common. The most polluted section was S1 (32.8 ± 16.7 item/m^3), whereas the least polluted section was S2 (3.5 ± 4.9 items/m^3).

The Ukrainian section was not sampled in the following year (2022), but the main tributaries were involved in the study. The MP content of the water samples almost doubled, as the MPC ranged from 4 to 63 item/m^3 (MPC$_{mean}$: 23.7 ± 15.8 item/m^3). The average MPC of the Tisza (22.4 ± 14.8 item/m^3) was less than that of the tributaries (27 ± 19 item/m^3). This year, the Zagyva River was the most polluted tributary (63 item/m^3). At seven sites, the MP pollution of the water was strong or worse (≥ 30 item/m^3), thus the frequency of the polluted sites increased to 25% compared to the previous 19%. The greater contamination of the water system is shown by the fact that the number of slightly contaminated sites almost halved (4 sites). The spatiality of the pollution changed, as most of the previously strongly or heavily polluted sites became less polluted (sites "i" and "v"), and high MPCs appeared at new locations (sites "f", "u", "x" and "y") reflecting 2.6–6-fold increase. The formerly least polluted S2 section became the most polluted (30.5 ± 20.5 item/m^3), as its MPC increased by 8.7 times. The least polluted section became S3

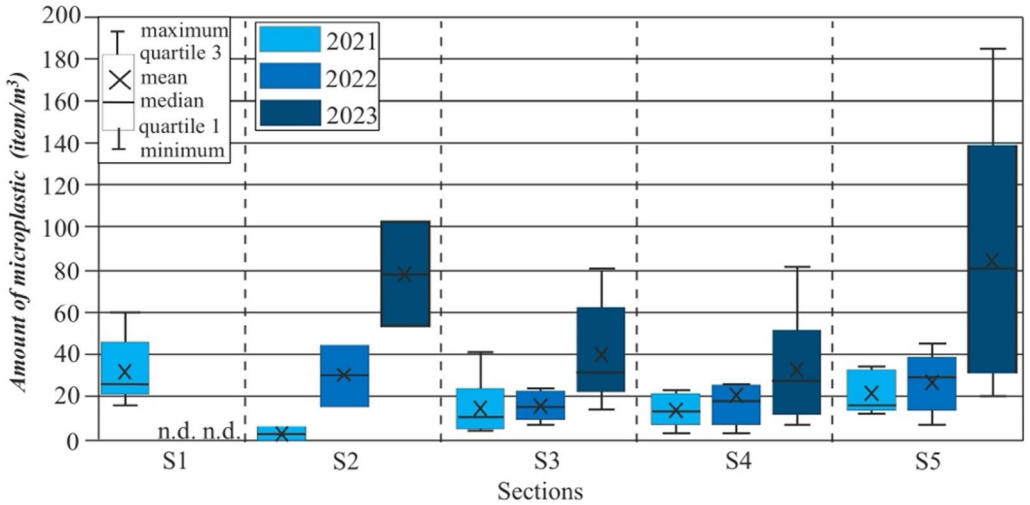

Fig. 4 Microplastic content of the sections of the Tisza River over the three survey years

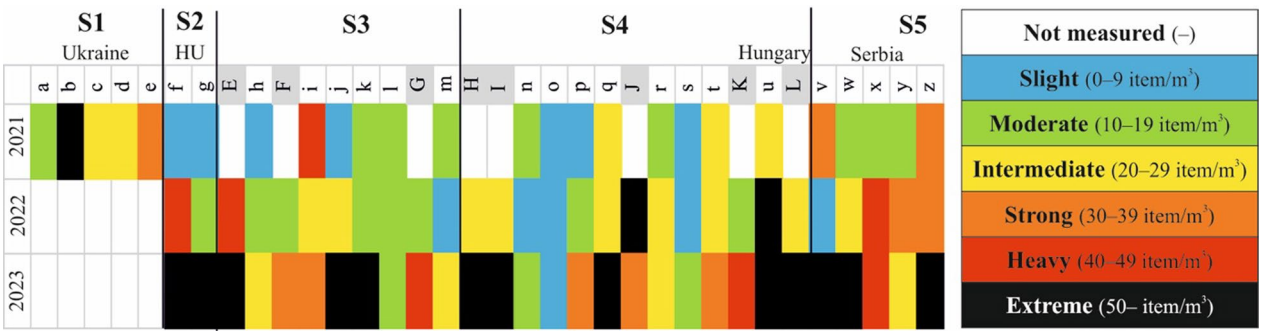

Fig. 5 Changes in microplastic pollution on sampling sites between 2021 and 2023. Sampling sites on the Tisza: a–z; sampling sites in the tributaries: E–L (and grey background)

(16.5 ± 6.6 item/m^3), even though its MPC increased by 25% compared to the previous year.

In the last survey year (2023), the MPC of the water almost doubled. The MPC ranged between 8 and 196 item/m^3, with an averaging of 57 ± 44.8 item/m^3. The average MPC of the Tisza (52 ± 41.6 item/m^3) was again less than that of the tributaries (70.3 ± 53.2 item/m^3), but in 2022 the tributaries were just more polluted by 20%, now it increased to 35%. All tributaries became at least strongly polluted, half of them became extremely polluted by MPs (Szamos: 56 item/m^3; Sajó: 196 item/m^3; Hernád: 77 item/m^3; and Maros: 73 item/m^3). The greatest increase was measured on the Tisza at site "v", where the MPC increased from 8 item/m^3 to 184 item/m^3 by 2023. Among the tributaries, the site on the Sajó River ("I") showed the greatest annual increase in MPC from 23 item/m^3 to 196 items/m^3. The overall increase in MPC is well reflected by the fact that the number of strongly or more polluted sites increased to 21 (75% of all sites), and the most frequent pollution category became "extreme" on 13 sites (46%). The MPC on these sites increased from 50% to 23 times (Figs. 4, 5). In 2023, there were just four sites where the pollution was slight or moderate (≤19 item/m^3) and none appeared on the tributaries. Only two sites reflected MPC decrease compared to the previous year: site "J", where MPC decreased by almost 50% (but remained strongly polluted), and site "y", where MPC decreased by more than 60%.

Considering the section-scale changes by 2023, the greatest increase in MPC was measured in section S5, where the mean MP pollution tripled (84.6 ± 62.8 item/m^3), and the section became the most polluted part of the Tisza. The lowest pollution (33.5 ± 25.1 item/m^3) and lowest variability were detected in section S4. Considering longitudinal changes, a steady decrease in MP pollution was observed from section S2 to S4.

Hydrological background and suspended sediment transport conditions during the longitudinal (spatial) surveys

Annual samplings along the Tisza and its tributaries were carried out at almost the same water levels each year (Fig. 6A). The annual longitudinal surveys were performed during summer low-water stages; higher stages appeared only in the impounded sections.

The daily water level changes were between −8 and + 17 cm. The arrival of small flood waves was presented by rising stages (at site "r": H_1: 17 in 2021; or on the Maros, at site "L": H_1: 17 cm in 2022), whereas the intensively falling stages refer the previous passing by of a flood wave (at site "t": H_1: −6 cm in 2023).

The stage changes three weeks before sampling (Fig. 6B) show greater variations (10–600 cm), referring to the passing of flood waves. Hydrologically, the most active year was 2023, when the greatest stage changes appeared. The highest flood waves were recorded on the Tisza at site "p" (H_{21}: 399 in 2021 and H_{21}: 218 cm in 2022); just downstream of the Kisköre Dam. Thus, these flood waves were probably artificially generated by opening the dam's gates to supply water for the downstream reach. The tributaries were also very active in 2023, as flood waves developed on most northern and northwestern sub-catchments. The largest was recorded on the Sajó (site "I", H_{21}: 600 cm). In the impounded sections (sites "k–o" and "t–y"), these flood waves gradually terminated, and the flood waves smoothened between (e.g., at the site "o" the H_{21} was never greater than 20–33 cm): 218–575 cm.

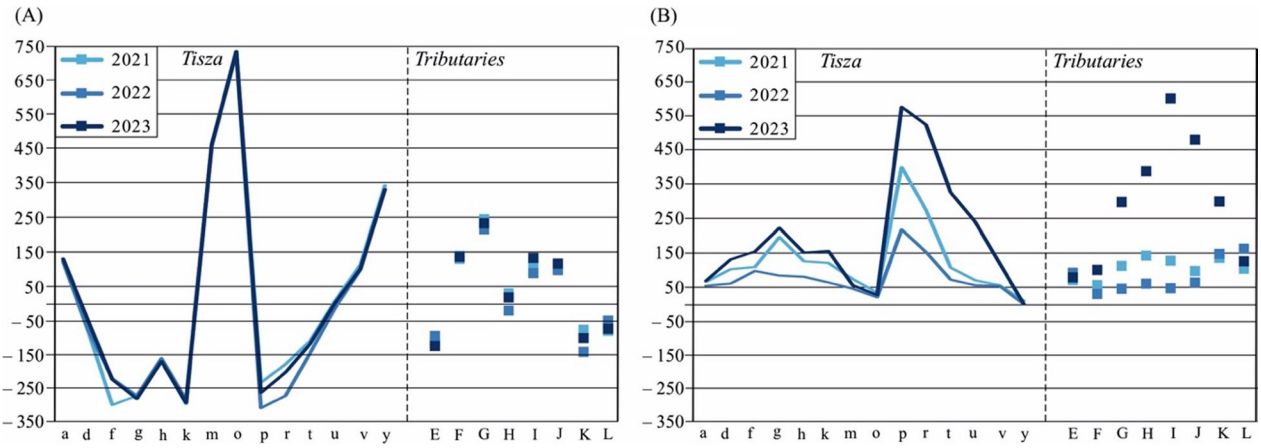

Fig. 6 The water stages on the sampling days were very similar during the three years (**A**). The absolute water stage changes in three weeks prior to sampling represent the existence of small flood waves in the water system (**B**)

Table 2 (A) Spearman rank order correlation coefficients between microplastic (MPC) and suspended sediment concentrations (SSC), concentrations, and daily water stages (H_0) for the Tisza over three consecutive measuring years (2021, 2022, and 2023), and (B) for the main tributaries (2022–2023)

	2021			2022			2023		
	MPC	SSC	H_0	MPC	SSC	H_0	MPC	SSC	H_0
(A) Tisza River									
MPC	1.0			1.0			1.0		
SSC	−0.26 ($p=0.36$)	1.0		−0.51 ($p=0.09$)	1.0		0.53 ($p=0.08$)	1.0	
H_0	0.46 ($p=0.10$)	−0.24 ($p=0.42$)	1.0	−0.25 ($p=0.44$)	0.06 ($p=0.86$)	1.0	−0.45 ($p=0.15$)	−0.59 ($p=0.04$)	1.0
(B) Tributaries									
MPC	n.a			1.0			1.0		
SSC				0.92 (p = 0.003)	1.0		−0.21 (p = 0.61)	1.0	
H_0				−0.24 (p = 0.56)	0.0 (p = 1.0)	1.0	−0.19 (p = 0.65)	−0.24 (p = 0.57)	1.0

Considering all 3 years, the mean SSC of the Tisza was 51.3 ± 28.5 g/m^3, but for the tributaries, it was much higher (116.9 ± 57.9 g/m^3). Similar values were measured between the years (Table 2), though slightly higher SSC was detected on the tributaries in 2023 (123.8 ± 58.9 g/m^3). Along the Tisza, the highest SSC (site "f": 139 g/m^3) was measured in 2023, when small flood waves propagated in the system. The lowest SSC was measured in 2022 on-site "u" (19 g/m^3), probably related to the more even hydrology (missing floods). For the tributaries, the highest value (250.7 g/m^3) was measured on the Szamos River (site "E") also in 2023, while the lowest value (29.3 g/m^3) was measured on the Körös River (site K) in 2022.

Correlation between hydrology, suspended sediment, and microplastic concentrations based on annual measurements along the river system

The longitudinal data on the water stage on the day of the survey (H_0), SSC, and MPC over the three years (2021–2023) revealed a stronger correlation between these variables in the Tisza than in its tributaries (Table 2). In general, there is a negative correlation between H_0 and both MPC and SSC in the Tisza and its tributaries across the years. The highest negative correlation coefficients were observed in 2023. However, a positive correlation was observed in the Tisza between H and MP concentration in 2021 ($\rho=0.46$) and between H and SSC in 2022 ($\rho=0.06$). The statistical analysis between the other hydrological parameters (i.e., H_1, H_{21}) and SSC and MPCs did not show significant correlations.

The correlation between SS and MP concentrations is stronger than their relationship with H in both the Tisza and its tributaries. Typically, there is a weak to strong negative correlation between SS and MP concentrations in both the Tisza and its tributaries. Notably, a strong positive correlation ($\rho=0.53$) was detected in the Tisza in 2023, and a very strong positive correlation ($\rho=0.92$) was observed in the tributaries in 2022.

Based on the Kruskal–Wallis H and post hoc test analysis, the SSC and MPC showed a statistically significant difference (higher concentrations) in 2023 compared to 2021 and 2022 in the Tisza and compared to 2022 in the tributaries (Fig. 7). Notably, there was an exception for SSC in the tributaries, which did not reveal a statistically significant difference between the survey years (2022 and 2023). Also, no significant difference was observed in the SSC and MPC in the Tisza between 2021 and 2022.

When comparing SSC and MPC between the Tisza and its tributaries in 2022, the SSC in the tributaries was statistically significantly different (higher concentrations) than its counterpart in the Tisza, while no difference was observed in the MP concentration. In 2023, no significant differences were observed in these variables (i.e., SSC and MPC) between the Tisza and its tributaries.

Microplastic and suspended sediment clouds

The frequent monitoring at one site ("u": Mindszent) revealed that the MPC is not uniform across various hydrological conditions. During medium flood waves, the SSC and MPC rapidly increased, and their peaks usually coincided with the flood peak. Remarkably, the magnitude of floods was not associated with the SSC and MPC. Typically, the first flood wave following a prolonged low-stage period had higher SS and MP loads than subsequent waves. On the contrary, the SSC and MPC were low during low stages. However, they had common peaks related to minor flood waves, but in some cases, these peaks appeared without any changes in the water level.

These temporal changes refer to the existence of medium-scale SS and MP clouds. These clouds were detectable on Sentinel images. Thus, longer channel

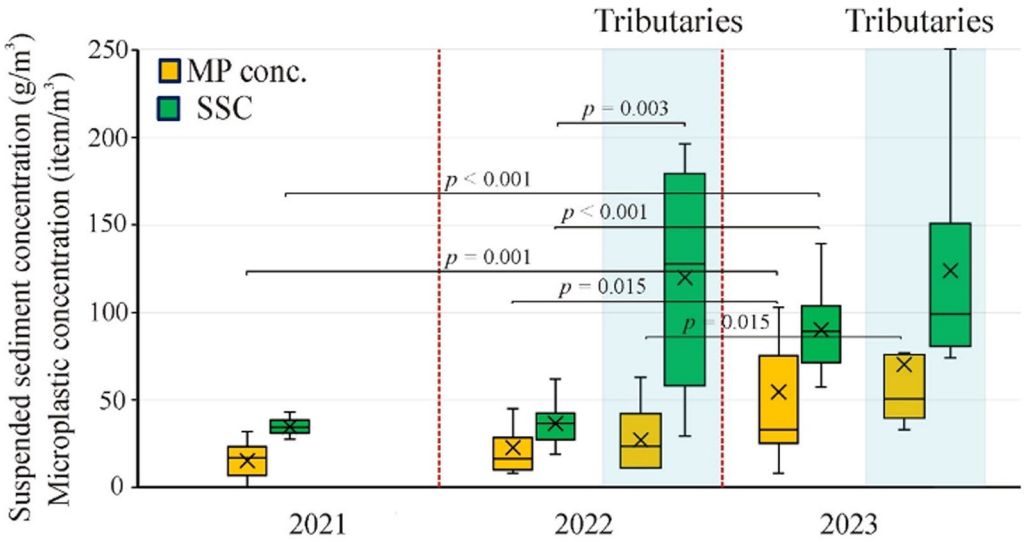

Fig. 7 Box plots for the suspended sediment (SSC) and microplastic (MPC) concentrations in the Tisza (2021–2023) and the tributaries (2022–2023). *P*-values are included only for statistically significant pairs

sections could be studied in detail. At low water stages, the SS and MP clouds were distinguishable (Fig. 8). For example, before the sampling on August 2, 2021, a small flood wave had passed, and the measurement was made at the end of its falling limb (H_1: 5 cm H_{21}: 70 cm) (Fig. 8A). The modelled SSC (34–43 g/m^3) and MPC (9–13 item/m^3) were not evenly distributed. Three major SS and MP clouds were visible in the 8 km-long presented section; their peaks were spaced about 2.5–3 km apart. Between the clouds, water bodies with less SS and MP were found, with a length of ca. 1 km. The clouds had different SSC and MPC (Fig. 8), but a less sediment-rich water body was always observed between them. The MPC appeared in less distinct waves than the SSC, but its pulses were also visible. The validity of the modelled data was shown by the fact that a similar MPC (13 item/m^3) was measured at this time.

The SS and MP clouds were also observed in the rising and falling limbs of flood waves (Fig. 8). On the selected rising limb of a flood wave (May 4, 2021), the water level changed dynamically (H_1: 6 cm, H_{21}: 161 cm) (Fig. 8B). In this hydrological situation, the differences between SSC and MPC clouds were characteristic, as, at the peak of the clouds, the SSC reached 48–53 g/m^3 and the MPC 35–37 item/m^3. On the contrary, the river had less SSC (36–40 g/m^3) and MPC (30–31 item/m^3) between the clouds. At this time, three long (3–5 km) clouds followed each other quickly due to the higher water velocity. The SS clouds were more pronounced during the rising limb, whereas the MPC had flattening waves.

In contrast, in the falling limb (e.g., on June 3, 2022), the stages were less variable (H_1: –3 cm, H_{21}: 52 cm) (Fig. 8C). In this hydrological situation, the SSCs and MPCs of the river were more homogeneous. The peaks of the clouds (SSC: 35–42 g/m^3; MPC 12–13 item/m^3) were more similar to the clearer water mass in between them (SSC 30–31 g/m^3; MPC 8–10 item/m^3). The length of the clouds was just 0.2–0.5 km, and in the studied section 7, small clouds followed each other much more irregularly (0.5–1.5 km) than before.

Tributaries can create SS and MP clouds (Fig. 9). For example, in August 2023, a bankfull flood wave propagated along the Sajó–Hernád river system immediately before the sampling. The tributaries had great stage changes (H_1: –3 cm, H_{21}: 600 cm), while the water level of the Tisza slightly changed (H_1: –1 cm, H_{21}: 55 cm). The water of the tributary contained 92.6 g/m^3 suspended sediments and 196 item/m^3 microplastics upstream of the confluence. The Tisza transported only 62 g/m^3 suspended sediments and 28 item/m^3 microplastics. Despite the increased discharge of the tributary, the SSC of the Tisza increased only slightly below the confluence (85 g/m^3), and the MPC decreased (8 item/m^3), as the discharge of the Sajó was neglectable compared to the Tisza's. However, mixing the two waters created sediment clouds that started to move downstream. The SSC reached 50–54 g/m^3 in these clouds and MPC 24–26 item/m^3. Therefore, three sediment clouds were observed downstream of the confluence along the 6 km-long section, but as presented in the previous paragraph, they were not well-marked because of the falling stages.

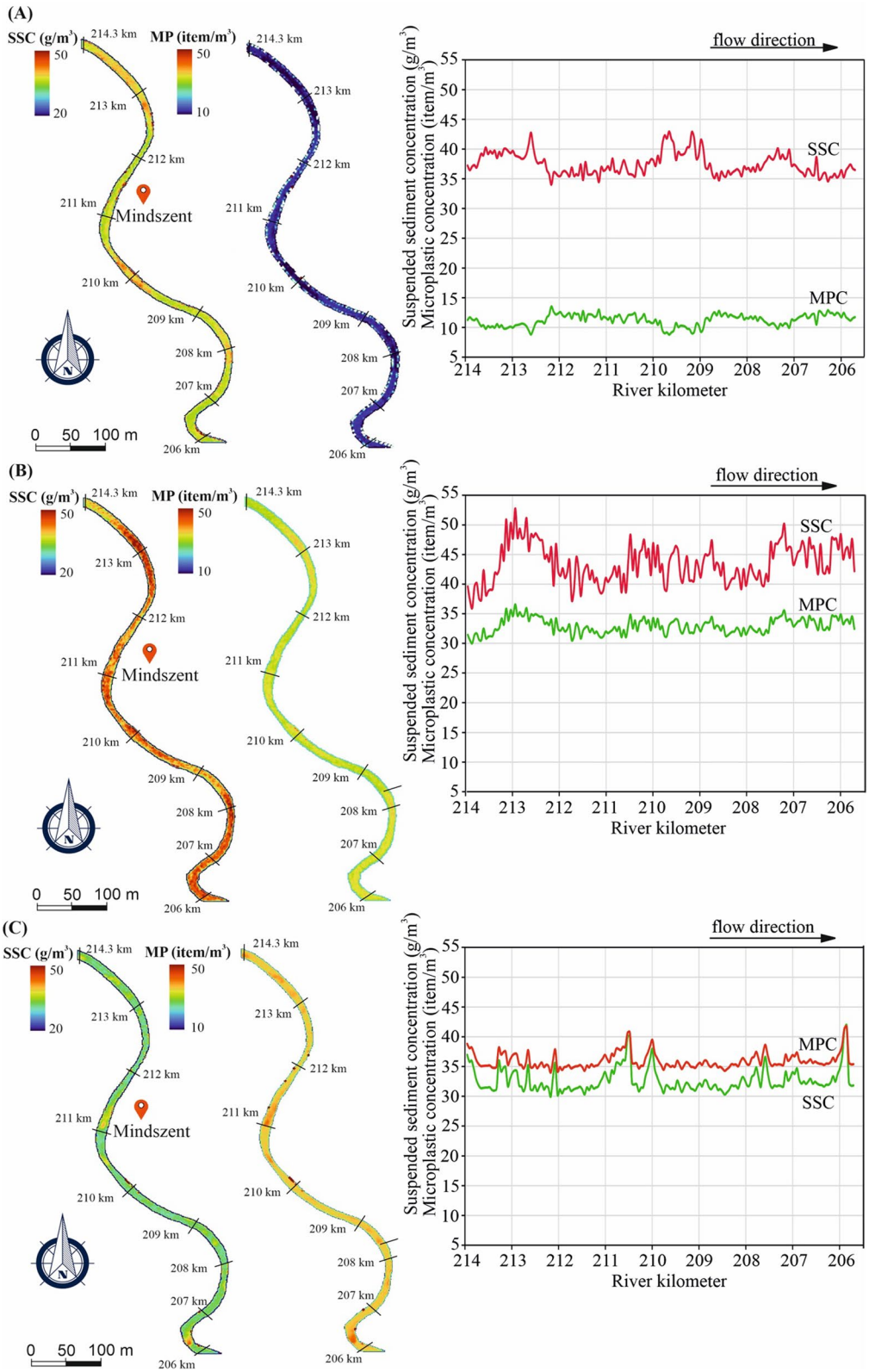

Fig. 8 Modelled suspended sediment (SS) and microplastic concentration (MP) at the sampling site Mindszent ("u"). The SSs and MPs were transported in clouds where they had higher concentrations. Changes in suspended sediment and microplastic concentrations along the centerline of the channel during low stage (**A**), rising limb (**B**), and falling limb (**C**)

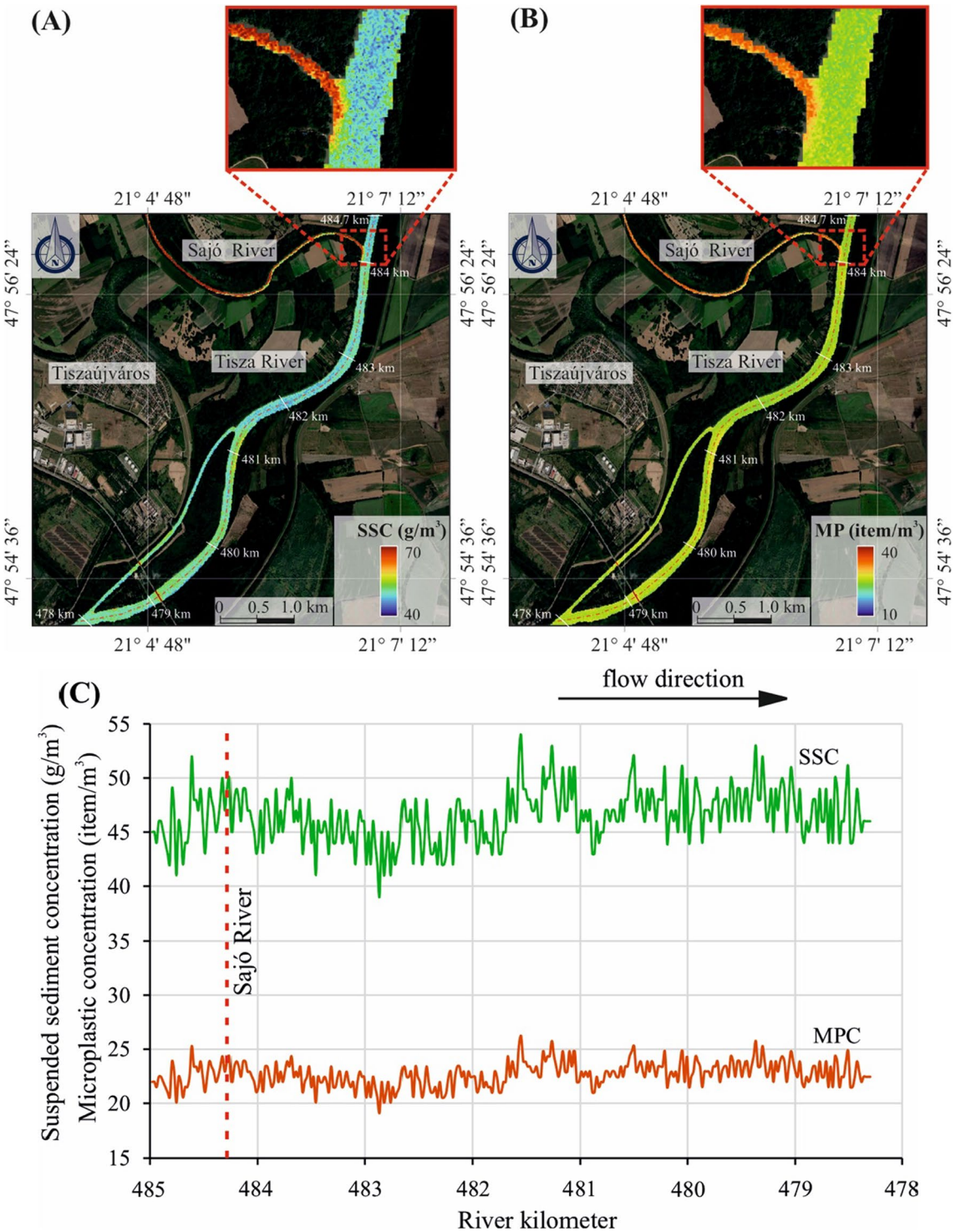

Fig. 9 Modelled suspended sediment (SS) (**A**) and microplastic concentration (MP) (**B**) at the confluence area of the Sajó Hernád Rivers after a bankfull flood of the tributary and low stage on the Tisza River in August (2023). Changes in suspended sediment and microplastic concentrations along the centerline of the channel in August 2023 (**C**)

Discussion

Temporal changes in hydrology, suspended sediment, and microplastic concentrations

Our intra-annual, frequent (5-day return), and two-year-long measurements proved that hydrological conditions significantly impact SSC and MPC in a river. Ockelford et al. [50] found a similar positive correlation between SSC and hydrological changes. A stronger correlation was found for surface SSC with hydrological parameters than for MPC, suggesting that hydrological factors are more important influencing factors for the transport of SS than the MP.

This difference could be explained by the dissimilarities in the sources and transport of SS and MP. Suspended sediment can either enter the river during high rainfall events through surface run-off and soil erosion [65] or through vertical and horizontal erosion of the channel [56], thus, by processes that are strongly related to hydrology. In contrast, MP particles could be washed off from the catchment, for example, by soil erosion of soils treated with sewage sludge, by run-off from landfills or road surfaces [5, 20, 26, 40]. However, the main source of MPs is treated or untreated wastewater discharged directly into rivers [15, 17, 18, 58, 66], resulting in the completely independent spatial and temporal distribution of MP pollution from run-off conditions. Besides, the different shape, grain size, degradation, and density of MP grains [64] influence the time they remain suspended in the water column and the rate of their sedimentation [8, 25]. Besides, the MP particles could get more easily mobilized and be transported away than natural sediment grains [7, 64].

The water level (and thus discharge) changes strongly influence the temporal variation of SSC and MPC. During low water stages, SSC and MPC are only slightly correlated. Similar negligible correlations were observed by Chen et al. [8], but Wu et al. [67] found a negative correlation, showing that MP particle abundance was higher during low water periods (4–25 items/L) than at higher water stages (3–10 items/L). The slight correlation between SSC and MPC could be explained by their different sources. During low stages, most of the water discharge of the Tisza originates from groundwater [38], but MPs come from wastewater effluents. However, SS does not originate from these sources. Besides, the low flow velocity (Tisza: $\leq$ 0.02 m/s) and stream power during low stages stimulate the deposition of both SS and MP grains but at a different rate [64], contributing to lower SSCs and MPCs.

During the rising limb of flood waves, the Tisza carries a large amount of SS and MP particles, and a strong positive correlation was observed between SSC and MPC. This suggests that new, common sources of SS and MP associated with run-off and accelerated flow velocity emerged in the hydrological system [46]. Floods originate from run-off in mountainous and hilly sub-catchments, mobilizing material from soils, slopes, and artificial surfaces. Therefore, not only SS sources but also new MP sources become active. Besides the increased discharge, the higher flow velocity and the more turbulent flow mobilize both the deposited SS and MP grains from the riverbed, increasing their concentration.

The weakest correlation between SSC and MPC was observed in the falling limb of flood waves when the transport capacity of the river decreases promoting deposition [49]. It could be explained by the different deposition rates of SS and MP particles, explained by their different shapes [15, 58], and densities [25].

Besides the phases of flood waves, their temporality is also important. Historically, one or two large floods appeared on the Tisza in springtime. Today, the flood season starts in winter, and 4–5 medium flood waves pass until the end of spring. The studied flood waves had different SSC and MPC, as the first flood wave always had higher concentrations. It could be explained by the importance of event sequence [62], as the first flood mobilizes natural sediments and MP particles more effectively from the bottom of the channel, so their concentration during the first wave is always higher than during the next similar or even higher flood waves.

Fluvial systems are complex, as at a given moment, various numbers of flood waves could co-exist, and they gradually move downstream. The spatiotemporal pattern of the flood waves could be quite complex during heavy rainfall events in summer. In this season, some sub-catchments could be very active, while others have very low stages. Thus, the low stages could be disrupted by flood waves generated in a tributary, especially on the main river. This mosaic spatial pattern caused complex MPC and SSC patterns through a survey. For example, just before our measurement in 2023, a cyclone initiated 300–600 cm high flood waves on the northern and northwestern tributaries (Bodrog, Hernád–Sajó, Zagyva, and Körös). These flood waves mobilized the SS and MP grains; thus, these tributaries had high MPCs despite the falling limb of the flood waves. However, they only slightly or moderately increased the MPC of the main river due to their low discharges related to the main river.

Microplastic pollution of the Tisza and its spatial changes

The MP pollution has a clear increasing temporal trend based on comparing the results of the three-year monitoring along the Tisza. Most of the particles (94–97.4%) were fibers. The fibers probably originated from wastewater, especially because in some regions of the catchment, the wastewater treatment is quite low. The importance of

treated and untreated wastewater in MP pollution was also highlighted in many rivers [15, 17, 18, 36, 58, 59, 66]. However, some recent studies have identified fibers in locations far from wastewater treatment plants [22], and others have shown weak correlation between MPs to WWTP proximity [30, 32]. The mean MPC of the entire Tisza during the low stage sampling was 19 ± 13.6 item/m^3 (2021), 22.4 ± 14.8 item/m^3 (2022), and 52 ± 41.6 item/m^3 (2023). The tributaries can act as SS conveyors [44], therefore, they usually also transport considerably higher MPCs (2022: 27 ± 19 item/m^3 and 2023: 70.3 ± 53.2 item/m^3). However, during higher stages, the MP pollution of the Tisza (at one point) was 122–124 item/m^3. It suggests that MP pollution of the Tisza could be considered as medium to high compared to other large European rivers. For example, on the Elbe (Germany), the MPC was 5.57 ± 4.33 item/m^3 [58], and in the Seine (France), it was 0.28–0.47 item/m^3 [16]. However, the differences in sampling methodology and environmental conditions could weaken the comparison (Table 1), and it should also be noted that our data reflect low stages when the MPC is lower.

The pollution status of the sections (S1–5) of the Tisza gradually became worse over the three years, having the greatest increase in 2023. The MP pollution increased at 93% of the sampling sites and remained almost the same at two sites. The increase in MPC was particularly high in sections S2 and S5, which represent the Hungarian section of the Upper Tisza and the lowermost Serbian sections. Wastewater treatment is relatively poor in these areas, as only 61–78% of the settlements in Hungary are connected to the sewage system, and 71–91% of the collected wastewater is treated [34]. The situation is even worse in Serbia, as only 16% of the households are connected to the sewage system, and 67.2% individually collect the wastewater in digestive pits [19]. According to informal sources, the untreated sewage is drained directly to the Tisza or to canals joining the Tisza ultimately.

Suspended sediment and microplastic clouds

Our measurements on SSC and MPC suggest that the SS and MP particles are transported in clouds, where the SSC and MPC are higher than in between them [7]. The existence of SS clouds was also proven by Gilvear and Bryant [23], who found that there is a large variability in SSC (0–300 mg/L) within a short reach (0.5 km), as an SS-rich water body is not evenly mixed within a clearer water body. The SS clouds are connected to tributaries, as the rivers could carry different sediment loads, and the water mixing creates clouds. Such clouds related to a tributary were presented by Mohsen et al. [47] over a 4 km reach downstream of a confluence, while Maurice-Bourgoin et al. [43] detected them along 25 km. Lane et al. [37] found that complete mixing often takes very long distances (ca. 100 km) in large rivers.

Our modelled results show that clouds with larger SSC and MPC are located further apart during low stage periods, while during floods, shorter clouds could be identified following each other quickly. However, less variability in MPC was detected than in SSC, probably because the shear stress of the MP particles is lower than SS grains [64], thus, some of the MP particles could be mobilized earlier than natural SS particles and may remain in suspension longer due to their light density and irregular shape.

At low water stages, due to reduced water velocity, SS and MP clouds move slowly. Sometimes 14–28 h pass between two consecutive SSC and MPC peaks (Table 3). During flood waves, the increased flow velocity decreases time between MP peaks for 30–40 min.

Microplastic monitoring considerations

On the one hand the frequent, two-year-long monitoring at one site enabled us to reveal the hydrological background of SS and MP transport. On the other hand, the repeated measurements along the river made it possible to evaluate their spatial changes. When planning MP monitoring, we recommend considering the hydrological characteristics of a river: the duration and level of floods and their event sequence based on the historical regime data. In case of repeated measurements, it is offered to perform the sampling at the same hydrological situation (e.g., rising limb, peak or falling limb of a flood) to make the data comparable. It is also important to record (and

Table 3 Main characteristics of sediment clouds transporting large amounts of suspended sediment and microplastics during various stages based on the acquisition of Sentinel images

Characteristic stage (example)	Flow velocity (m/s)	Cloud characteristics	
		Distance of the peaks (km)	Estimated time between two peaks
Low stage (Aug. 2, 2021)	0.02	1–2	14–28 h
Rising limb of a flood (May 4, 2021)	0.25	0.4–0.6	27–40 min
Falling limb of a flood (June 3, 2023)	0.1	0.8–1	2.2–3 h

publish) the hydrological conditions during the measurement for comparability.

Our data suggest that the low stage and flood peak MPCs are fundamentally different, as much higher MPCs could be measured during floods. It is because the MP sources of the catchment are connected to the river during heavy rainfalls and partly because during a flood, MP clouds are more likely to be sampled due to the fast movement of clouds. However, sampling during floods is quite difficult. On the contrary, during low stages, sampling is easy. However, the complex spatiotemporal activity of the sub-catchments results in a mosaic pollution pattern, and the clouds are located farther from each other. Therefore, if the sample is from a higher MPC cloud or water with lower MPC, one can get quite random data.

Tributaries act as conveyor belts for SS and MP, and their role can be particularly important when they flood while the main river is in a low stage. Their remobilized sediments (including SS and MP grains) could be the main sediment supply for the main river; however, they can present complex mixing patterns [46]. Therefore, the sampling site should be carefully chosen downstream of tributaries, as the sampled water body could represent the waters of the joining rivers with different pollution degrees.

Finally, it is important to note that the method developed for the indirect estimation of MPC using SSC as a proxy showed high accuracy, especially when applied to the rising limb of floods ($R^2 = 0.17–0.88$). It is a very useful tool to detect MPC changes along longer sections and to understand the mixing patterns and clouds of MP and SS particles. However, this method is limited by the width of the river (vs. pixel size of the image) and very low MPCs. The color and SSC of each river are different; therefore, it is highly advised to validate our model by frequent at-a-site monitoring of SSC and MPC.

Finally, if the contamination during the sample preparation is higher than 2–7%, it is advised to consider collecting a higher volume of samples (several m^3) to eliminate the contamination effect in the lab.

Conclusions

The strength of this study is that from the hydrological point of view, our measurements are unique, as (1) the temporal changes were analyzed based on frequent (5-day) and long (2 years) monitoring; (2) the spatial changes were revealed all along the 745 km length of Tisza for three years; (3) and the spatiotemporality of the MPC was modelled using the SSC as a proxy, based on Sentinel images.

It must be highlighted that throughout the surveyed period, the MPC steadily increased, and more and more sites became polluted. The MP highly depends on the hydrological regime, as flood waves transport higher MPC. Since the tributaries act as conveyors, these flood waves appear in the system as clouds or pulses. It is also important to note that there is no straightforward relationship between hydrology and MPC due to the influence of the "event sequence". Thus, always the first flood wave increases the SSC and MPC the most because the great stream power is combined with a higher amount of mobilizable sediment from the bottom, deposited previously during low stages.

Although a growing number of studies investigate the MP pollution of rivers, the case studies rarely report the hydrological conditions during sampling. Besides, most studies provide just a snapshot of MP contamination at a given point or time; thus, their results are hardly comparable because of the different environmental (hydrological) conditions. Our study proved that deeper knowledge of the hydrological driving factors of MP transport, deposition, and mobilization is needed.

The analysis revealed that hydrology (e.g., low stages, floods and event sequence) fundamentally influences the MP transport of a river. Besides, the hydrological activity of tributaries creates complex spatial patterns in the transport dynamics of SS and MP. The SS and MP particles are not transported in a homogenous concentration but in clouds. Therefore, during sampling, special attention should be paid to the sampling circumstances, whether the sample is taken from a cloud (which could be checked immediately with drones) or whether the upstream tributary is already mixed with the water of the main river. We also suggest using ≥ 1 m^3 water samples to eliminate the effects of small SSC and MPC clouds (waves) and procedural contamination.

The take-home messages of our study are that (1) continuous monitoring rather than single-site measurement is needed to understand temporal and spatial changes, and (2) the hydrological history of a river plays a crucial role in the actual MPC; therefore, it must be considered. To ensure the repeatability of the measurements, it is worth sampling in similar hydrological situations and considering the excess SSC and MPC transported by tributaries and point sources.

Appendix A

Characteristics of the sections of the Tisza River

The upper section of the Upper Tisza (S1: 946–927 river km) is located in the Carpathian Mountains in Ukraine (Fig. 1), where the river is incised into a valley with steep valley slopes. The river has a great slope too (20–50 m/km) and high flow velocity (2–3 m/s) [38]. The settlements are located in the narrow valley. Most sewage is untreated and drained directly into the Tisza, and the

municipal waste is often stored along the bank lines and washed directly into the Tisza during rainfall events (Tarpai, 2011).

The sub-catchments of the lower section of the Upper Tisza sub-basin (S2: 927–688 r km) are in Romania, Ukraine, and Hungary. The slope of the Tisza decreases from 110 cm/km to 13 cm/km, and the flow velocity is only 1.0 m/s [38]. The Szamos (Q_{mean} = 120 m^3/s) and the Kraszna (Q_{mean} = 5 m^3/s) spring in Romania and join the Tisza at the end of the section. The other tributaries have much smaller discharges and mostly originate in Ukraine. The floodplains of the rivers are confined by artificial levees in the lowland areas; thus, no sediment or wastewater can enter directly into the water system. In Ukraine, sewage and waste disposal are inadequate, even in the larger sub-catchment towns (Tarpai, 2013). The situation is similar in Romania, with an average of 41% of households connected to the public sewage system but only 5–15% in rural areas [55].

The sub-catchments of the Middle Tisza's upstream section (S3: 688–484 r km) are located in the mountainous and hilly areas of Slovakia and the lowlands of Hungary. The slope of the Tisza decreases to 3–6 cm/km, and the flow velocity drops to 0.1–0.5 m/s [38]. The water and sediment transport are controlled by the Tiszalök Dam, which impounds the river up to the bankfull level on a 75 km-long section (between "k" and "m" sites). In this section, the Bodrog (Q_{mean} = 124 m^3/s) and the Sajó–Hernád (Q_{mean} = 65 m^3/s) river systems transport large amounts of water and sediment to the Tisza [38]. Slovakia and Hungary have good waste and wastewater management practices, but still, significant physical (e.g., municipal waste, PET) or chemical pollution affects the rivers from time to time [27].

The lower section of the Middle Tisza (S4: 484–177 r km) is characterized by an even lower slope than previously, as the slope is only 1–3 cm/km. Therefore, the flow velocity is only 0.1–0.5 m/s [38]. The Kisköre Dam impounds the Tisza along 115 km, up to the Tiszalök Dam (between sites "m" and "o"). Its reservoir impounds the river above the former floodplain level, forming the "Tisza Lake" (127 km^2). Among the tributaries, the Körös (Q_{mean} = 105 m^3/s) and the Maros (Q_{mean} = 160 m^3/s) rivers originate in Romania, while the Zagyva (Q_{mean} = 10 m^3/s) collects water from Hungary [38].

The Lower Tisza (S5: 177–0 r km) is almost entirely located in Serbia, and its catchment includes mostly flatland areas. The slope (1–0 cm/km) and velocity (0.0–0.2 m/s) of the Tisza are controlled by the operation of the Novi Becej Dam. It impounds the water along nearly 200 km of the Tisza up to the bankfull level (between sites "t" and "y"), so the impoundment affects even the downstream part of the S4 section up to the confluence of the Körös. The Serbian villages along the Tisza are among the least developed in sanitation, as only 25–30% of the households were connected to sewerage systems [60].

Acknowledgements
The authors are grateful to everyone who helped during the sampling, and for the Lower Tisza District Water Directorate (ATIVIZIG) for providing the hydrological data. Thanks to the anonymous reviewers for their valuable comments.

Author contributions
Conceptualization, T.K.; methodology, A.B. and A.M.; writing – original draft preparation, A.B.; writing – review and editing, A.B. and T.K.; visualization, A.B. and A.M.; project administration, T.K. All authors have read and agreed to the published version of the manuscript.

Funding
Open access funding provided by University of Szeged. The research was funded by the Hungarian Research Foundation (OTKA No. 134306 and ÚNKP-23-3 -SZTE-421– New National Excellence Program of the Ministry for Culture and Innovation from the source of the National Research, Development and Innovation Fund.) and University of Szeged Open Access Fund, Grant ID: 7047.

Availability of data and material
No datasets were generated or analyzed during the current study.

Declarations

Competing interest
The authors declare that there are no competing interests.

Author details
[1]Department of Geoinformatics, Physical and Environmental Geography, University of Szeged, 6722 Szeged, Hungary. [2]Department of Irrigation and Hydraulics Engineering, Tanta University, Tanta 31527, Egypt. [3]Independent Researcher, Horváth Gy. Str. 80, 6630 Mindszent, Hungary.

Received: 21 May 2024 Accepted: 30 July 2024
Published online: 11 August 2024

References

1. Andrady AL (2011) Microplastics in the marine environment. Mar Pollut Bull 62:1596–1605. https://doi.org/10.1016/j.marpolbul.2011.05.030
2. Anuar ST, Abdullah NS, Yahya NKEM, Chin TT, Yusof KMKK, Mohamad Y, Azmi AA, Jaafar M, Mohamad N, Khalik WMAWM, Ibrahim YS (2023) A multidimensional approach for microplastics monitoring in two major tropical river basins. Malaysia. Environ Res 227:115717. https://doi.org/10.1016/j.envres.2023.115717
3. ASTM (2007) Standard test method for determining sediment concentration in water samples. Pennsylvania, West Conshohocken, p 6
4. Balla A, Mohsen A, Gönczy S, Kiss T (2022) Spatial variations in microfiber transport in a transnational River basin. Appl Sci. https://doi.org/10.3390/app122110852
5. Bhardwaj LK, Rath P, Yadav P, Gupta U (2024) Microplastic contamination, an emerging threat to the freshwater environment: a systematic review. Environ Syst Res 13:8. https://doi.org/10.1186/s40068-024-00338-7
6. Bogárdi J (1971) Sediment transport of rivers (Vízfolyások hordalékszállítása). Budapest, Akadémiai kiadó, p 837
7. Bussi G, Darby SE, Whitehead PG, Jin L, Dadson SJ, Voepel HE, Vasilopoulos G, Hackney CR, Hutton C, Berchoux T, Parsons DR, Nicholas A (2021) Impact of dams and climate change on suspended sediment flux to the Mekong delta. Sci Total Environ 755:142468. https://doi.org/10.1016/j.scitotenv.2020.142468
8. Chen HL, Gibbins CN, Selvam SB, Ting KN (2021) Spatio-temporal variation of microplastic along a rural to urban transition in a tropical river. Environ Pollut 289:117895. https://doi.org/10.1016/j.envpol.2021.117895
9. Corami F, Rosso B, Bravo B, Gambaro A, Barbante C (2020) A novel method for purification, quantitative analysis, and characterization of

microplastic fibers using Micro-FTIR. Chemosphere 238:124564. https://doi.org/10.1016/j.chemosphere.2019.124564
10. Cowger W, Steinmetz Z, Gray A, Munno K, Lynch J, Hapich H, Primpke S, De Frond H, Rochman C, Herodotou O (2021) Microplastic spectral classification needs an open source community: open specy to the rescue! Anal Chem 93:7543–7548. https://doi.org/10.1021/acs.analchem.1c00123
11. Csépes E, Nagy M, Bancsi I, Végvári P, Kovács P, Szilágyi E (2000) The phases of water quality characteristics in the middle section of river Tisza in the light of the greatest flood of the century. Hidrológiai Közlöny 80:285–287
12. Csoma J, Szilágyi J, Zboray K (1967) Water, sediment and ice transport in the reservoir of the Tiszalök Dam (A tiszalöki duzzasztott tér víz-, hordalék- és jéglevonulási viszonyai). Vízügyi Közlemények 49:249–259
13. Dancey CP, Reidy J (2007) Statistics without maths for psychology. Pearson education, London
14. De Witte B, Devriese L, Bekaert K, Hoffman S, Vandermeersch G, Cooreman K, Robbens J (2014) Quality assessment of the blue mussel (Mytilus edulis): Comparison between commercial and wild types. Marine Pollut Bull 85:146–155. https://doi.org/10.1016/j.marpolbul.2014.06.006.
15. Di M, Wang J (2018) Microplastics in surface waters and sediments of the three gorges reservoir China. Sci Total Environ. https://doi.org/10.1016/j.scitotenv.2017.10.150
16. Dris R, Gasperi J, Tassin B (2018) Sources and fate of microplastics in urban areas: a focus on paris megacity. In: Wagner M, Lambert S (eds) Freshwater microplastics: emerging environmental contaminants? Springer International Publishing, Cham, pp 69–83
17. Eo S, Hong SH, Song YK, Han GM, Shim WJ (2019) Spatiotemporal distribution and annual load of microplastics in the Nakdong River South Korea. Water Res 160:228–237. https://doi.org/10.1016/j.watres.2019.05.053
18. Estahbanati S, Fahrenfeld NL (2016) Influence of wastewater treatment plant discharges on microplastic concentrations in surface water. Chemosphere 162:277–284. https://doi.org/10.1016/j.chemosphere.2016.07.083
19. EUROSTAT. Population connected to wastewater treatment plants. 1970 - 2021, https://doi.org/10.2908/ENV_WW_CON.
20. Faure F, Demars C, Wieser O, Kunz M, de Alencastro LF (2015) Plastic pollution in Swiss surface waters: nature and concentrations, interaction with pollutants. Environ Chem 12:582–591. https://doi.org/10.1071/EN14218
21. Fischer D, Käppler A, Fischer F, Brandt J, Bittrich L, Eichhorn K (2019) Identification of microplastics in environmental samples. Lab J Busi Web User Sci Indust. https://doi.org/10.26083/tuprints-00023031
22. Forrest SA, Vermaire JC (2023) Spatial distribution of microplastics in a large watershed: a case study of the Ottawa River watershed. Environ Monit Assess 195:645. https://doi.org/10.1007/s10661-023-11277-8
23. Gilvear D, Bryant R (2016) Analysis of remotely sensed data for fluvial geomorphology and river science. Tool Fluvial Geomorphol. https://doi.org/10.1002/9781118648551.ch6
24. Gonzalez-Saldias F, Sabater F, Gomà J (2024) Microplastic distribution and their abundance along rivers are determined by land uses and sediment granulometry. Sci Total Environ 933:173165. https://doi.org/10.1016/j.scitotenv.2024.173165
25. Hamdan AM, Lubis SS, Nazla CT, Jaswita D, Maulida Z, Munandar A, Hamdi H, Ardiansyah R, Khairuzzaman H (2023) Magnetic susceptibilities of suspended sediment and microplastic abundance in a tropical volcanic estuary. Reg Stud Marine Sci 61:102927. https://doi.org/10.1016/j.rsma.2023.102927
26. He D, Luo Y, Lu S, Liu M, Song Y, Lei L (2018) Microplastics in soils: Analytical methods, pollution characteristics and ecological risks. TrAC, Trends Anal Chem 109:163–172. https://doi.org/10.1016/j.trac.2018.10.006
27. Hungary Today. Sajó River Wildlife Endangered due to Polluted Mine Water from Slovakia. 2022 https://hungarytoday.hu/entire-wildlife-sajo-river-polluted-slovakia-mine-water-poison/. Accessed 16 May 2024.
28. Hurley R, Woodward J, Rothwell JJ (2018) Microplastic contamination of river beds significantly reduced by catchment-wide flooding. Nat Geosci 11:251–257. https://doi.org/10.1038/s41561-018-0080-1
29. Idowu GA, Oriji AY, Olorunfemi KO, Sunday MO, Sogbanmu TO, Bodunwa OK, Shokunbi OS, Aiyesanmi AF (2024) Why Nigeria should ban single-use plastics: excessive microplastic pollution of the water, sediments and fish species in Osun River Nigeria. J Hazard Mater Adv 13:100409. https://doi.org/10.1016/j.hazadv.2024.100409
30. Imbulana S, Tanaka S, Oluwoye I (2024) Quantifying annual microplastic emissions of an urban catchment: surface runoff vs wastewater sources. J Environ Manag. https://doi.org/10.1016/j.jenvman.2024.121123
31. Jaouani R, Mouneyrac C, Châtel A, Amiard F, Dellali M, Beyrem H, Michelet A, Lagarde F (2022) Seasonal and spatial distribution of microplastics in sediments by FTIR imaging throughout a continuum lake—lagoon-beach from the Tunisian coast. Sci Total Environ 838:156519. https://doi.org/10.1016/j.scitotenv.2022.156519
32. Kay P, Hiscoe R, Moberley I, Bajic L, McKenna N (2018) Wastewater treatment plants as a source of microplastics in river catchments. Environ Sci Poll Res 25:20264–20267. https://doi.org/10.1007/s11356-018-2070-7
33. Kim YH, Voulgaris G (2008) Lateral circulation and suspended sediment transport in a curved estuarine channel: Winyah Bay, SC, USA. J Geophys Res Oceans. https://doi.org/10.1029/2007JC004509
34. KSH. Statistical data on Hungary. https://map.ksh.hu/timea/?locale=hu. Accessed 27 Sep 2022.
35. Laermanns H, Reifferscheid G, Kruse J, Földi C, Dierkes G, Schaefer D, Scherer C, Bogner C, Stock F (2021) Microplastic in water and sediments at the confluence of the Elbe and Mulde rivers in Germany. Front Environ Sci. https://doi.org/10.3389/fenvs.2021.794895
36. Lahens L, Strady E, Kieu-Le T-C, Dris R, Boukerma K, Rinnert E, Gasperi J, Tassin B (2018) Macroplastic and microplastic contamination assessment of a tropical river (Saigon River, Vietnam) transversed by a developing megacity. Environ Pollut 236:661–671. https://doi.org/10.1016/j.envpol.2018.02.005
37. Lane SN, Parsons DR, Best JL, Orfeo O, Kostaschuk RA, Hardy RJ (2008) Causes of rapid mixing at a junction of two large rivers: Río Paraná and Río Paraguay, Argentina. J Geophys Res Earth Surface. https://doi.org/10.1029/2006JF000745
38. Lászlóffy, W. The Tisza River (A Tisza); Akadémiai Kiadó: 1982; p. 616 (in Hungarian).
39. Lechner A, Keckeis H, Lumesberger-Loisl F, Zens B, Krusch R, Tritthart M, Glas M, Schludermann E (2014) The Danube so colourful: a potpourri of plastic litter outnumbers fish larvae in Europe's second largest river. Environ Pollut 188:177–181. https://doi.org/10.1016/j.envpol.2014.02.006
40. Li J, Ouyang Z, Liu P, Zhao X, Wu R, Zhang C, Lin C, Li Y, Guo X (2021) Distribution and characteristics of microplastics in the basin of Chishui River in Renhuai. China Sci Total Environ 773:145591. https://doi.org/10.1016/j.scitotenv.2021.145591
41. Liu Y, You J, Li Y, Zhang J, He Y, Breider F, Tao S, Liu W (2021) Insights into the horizontal and vertical profiles of microplastics in a river emptying into the sea affected by intensive anthropogenic activities in Northern China. Sci Total Environ 779:146589. https://doi.org/10.1016/j.scitotenv.2021.146589
42. Mancini M, Serra T, Colomer J, Solari L (2023) Suspended sediments mediate microplastic sedimentation in unidirectional flows. Sci Total Environ 890:164363. https://doi.org/10.1016/j.scitotenv.2023.164363
43. Maurice-Bourgoin L, Quemerais B, Moreira-Turcq P, Seyler P (2003) Transport, distribution and speciation of mercury in the Amazon River at the confluence of black and white waters of the Negro and Solimões Rivers. Hydrol Proc 17:1405–1417. https://doi.org/10.1002/hyp.1292
44. Méndez-Freire V, Villaseñor T, Mellado C (2022) Spatial and temporal changes in suspended sediment fluxes in central Chile induced by the mega drought: the case of the Itata River basin (36°-37°S). J S Am Earth Sci 118:103930. https://doi.org/10.1016/j.jsames.2022.103930
45. MERI. Guide to Microplastic Identification; Marine and Environmental Research Institute: Blue Hill, ME, USA, 2017; p. 15.
46. Mohsen A, Kovács F, Kiss T (2023) Riverine microplastic quantification: a novel approach integrating satellite images, neural network, and suspended sediment data as a proxy. Sensors. https://doi.org/10.3390/s23239505
47. Mohsen A, Kovács F, Mezősi G, Kiss T (2021) Sediment transport dynamism in the confluence area of two rivers transporting mainly suspended sediment based on sentinel-2 satellite images. Water 13:3132. https://doi.org/10.3390/w13213132
48. Moshen A (2024) A multi-scale investigation of sediment and plastic pollution transport in the Tisza River applying remote sensing and machine learning: a hydrological perspective. University of Szeged, Szeged
49. Moskalski S, Floc'h F, Verney R (2020) Suspended sediment fluxes in a shallow macrotidal estuary. Mar Geol 419:106050. https://doi.org/10.1016/j.margeo.2019.106050

50. Ockelford A, Cundy A, Ebdon JE (2020) Storm response of fluvial sedimentary microplastics. Sci Rep. https://doi.org/10.1038/s41598-020-58765-2
51. Piehl S, Atwood EC, Bochow M, Imhof HK, Franke J, Siegert F, Laforsch C (2020) Can water constituents be used as proxy to map microplastic dispersal within transitional and coastal waters? Front Environ Sci. https://doi.org/10.3389/fenvs.2020.00092
52. Rackov J, Erceg T, Živković M, Teofilović V (2023) Spectroscopic analysis of microplastic fibers released during laundry washing cycle. Adv Eng Lett 2(2):71–79. https://doi.org/10.46793/adeletters.2023.2.2.4
53. Rákóczi, L. River processes in lowland rivers. In Proceedings of the IHP-V Project, Proceedings St. Petersburg Workshop, Paris, 1996; pp. 86–112.
54. Rodrigues MO, Abrantes N, Gonçalves FJM, Nogueira H, Marques JC, Gonçalves AMM (2018) Spatial and temporal distribution of microplastics in water and sediments of a freshwater system (Antuã River, Portugal). Sci Total Environ 633:1549–1559. https://doi.org/10.1016/j.scitotenv.2018.03.233
55. Romanian Water Association. Municipal Water and Wastewater Treatment Sector in the context of the EU Environmental Policy. https://www.yumpu.com/en/document/read/49722811/romanian-water-association. Accessed 27 April 2024).
56. Rusnák M, Kaňuk J, Kidová A, Šašak J, Lehotský M, Pöppl R, Šupinský J (2020) Channel and cut-bluff failure connectivity in a river system: case study of the braided-wandering Belá River, Western Carpathians. Slovakia Sci Total Environ 733:139409. https://doi.org/10.1016/j.scitotenv.2020.139409
57. Saadu I, Farsang A (2023) Plastic contamination in agricultural soils: a review. Environ Sci Eur 35:13. https://doi.org/10.1186/s12302-023-00720-9
58. Scherer C, Weber A, Stock F, Vurusic S, Egerci H, Kochleus C, Arendt N, Foeldi C, Dierkes G, Wagner M (2020) Comparative assessment of microplastics in water and sediment of a large European river. Sci Total Environ 738:139866. https://doi.org/10.1016/j.scitotenv.2020.139866
59. Schmidt C, Kumar R, Yang S, Büttner O (2020) Microplastic particle emission from wastewater treatment plant effluents into river networks in Germany: Loads, spatial patterns of concentrations and potential toxicity. Sci Total Environ 737:139544. https://doi.org/10.1016/j.scitotenv.2020.139544
60. Sefcsich, G. Public services (electricity, gas, heat water and waste) [Energiaszolgáltatás (áram, gáz, hő, víz, hulladék]. In Kistérségek életereje – Délvidéki fejlesztési lehetőségek, Gábrity Molnár, I.R., András, Ed.; Regionális Tudományi Társaság: Szabadka, 2006; pp. 191–192.
61. Shekoohiyan S, Akbarzadeh A (2022) The abundance of microplastic pollution along the Jajroud river of Tehran: estimating the water quality index and the ecological risk. Ecol Indic. https://doi.org/10.1016/j.ecolind.2022.109629
62. Talbot R, Chang H (2022) Microplastics in freshwater: a global review of factors affecting spatial and temporal variations. Environ Pollut 292:118393. https://doi.org/10.1016/j.envpol.2021.118393
63. Tran-Nguyen QA, Vu TBH, Nguyen QT, Nguyen HNY, Le TM, Trinh-Dang M (2022) Urban drainage channels as microplastics pollution hotspots in developing areas: a case study in Da Nang. Vietnam Marine Poll Bull 175:113323. https://doi.org/10.1016/j.marpolbul.2022.113323
64. Waldschläger K, Schüttrumpf H (2019) Erosion behavior of different microplastic particles in comparison to natural sediments. Environ Sci Technol 53:13219–13227. https://doi.org/10.1021/acs.est.9b05394
65. Walling DE (2005) Tracing suspended sediment sources in catchments and river systems. Sci Total Environ 344:159–184. https://doi.org/10.1016/j.scitotenv.2005.02.011
66. Wang J, Peng J, Tan Z, Gao Y, Zhan Z, Chen Q, Cai L (2017) Microplastics in the surface sediments from the Beijiang River littoral zone: composition, abundance, surface textures and interaction with heavy metals. Chemosphere 171:248–258. https://doi.org/10.1016/j.chemosphere.2016.12.074
67. Wu P, Tang Y, Dang M, Wang S, Jin H, Liu Y, Jing H, Zheng C, Yi S, Cai Z (2020) Spatial-temporal distribution of microplastics in surface water and sediments of Maozhou River within Guangdong-Hong Kong-Macao Greater Bay Area. Sci Total Environ 717:135187. https://doi.org/10.1016/j.scitotenv.2019.135187
68. Xu J-L, Thomas KV, Luo Z, Gowen AA (2019) FTIR and Raman imaging for microplastics analysis: state of the art, challenges and prospects. TrAC, Trends Anal Chem 119:115629. https://doi.org/10.1016/j.trac.2019.115629
69. Yang J, Monnot M, Sun Y, Asia L, Wong-Wah-Chung P, Doumenq P, Moulin P (2023) Microplastics in different water samples (seawater, freshwater, and wastewater): Methodology approach for characterization using micro-FTIR spectroscopy. Water Res 232:119711. https://doi.org/10.1016/j.watres.2023.119711
70. Yang R, Xu X, Xue Y, Zhang L, Guo J, Wang L, Peng M, Zhang Q, Zhu Y (2022) Horizontal and vertical distribution of microplastics in Gehu Lake. China Water Supply 22:8669–8681. https://doi.org/10.2166/ws.2022.401
71. Zhao W, Li J, Liu M, Wang R, Zhang B, Meng X-Z, Zhang S (2024) Seasonal variations of microplastics in surface water and sediment in an inland river drinking water source in southern China. Sci Total Environ 908:168241. https://doi.org/10.1016/j.scitotenv.2023.168241

Publisher's Note